Ordinary–extraordinary transition in dynamics of solutions of charged macromolecules

Murugappan Muthukumar[a,1]

[a]Department of Polymer Science and Engineering, University of Massachusetts, Amherst, MA 01003

Edited by Monica Olvera de la Cruz, Northwestern University, Evanston, IL, and approved September 8, 2016 (received for review July 25, 2016)

The occurrence of the ubiquitous and intriguing "ordinary–extraordinary" behavior of dynamics in solutions of charged macromolecules is addressed theoretically by explicitly considering counterions around the macromolecules. The collective and coupled dynamics of macromolecules and their counterion clouds in salt-free conditions are shown to lead to the "ordinary" behavior (also called the "fast" mode) where diffusion coefficients are independent of molar mass and polymer concentration and are comparable to those of isolated metallic ions in aqueous media, in agreement with experimental facts observed repeatedly over the past four decades. The dipoles arising from adsorbed counterions on polymer backbones can form many pairwise physical cross-links, leading to microgel-like aggregates. Balancing the swelling from excluded volume effects and counterion pressure with elasticity of the microgel, we show that there is a threshold value of a combination of polymer concentration and electrolyte concentration for the occurrence of the "extraordinary" phase (also called the "slow" mode) and the predicted properties of diffusion coefficient for this phase are in qualitative agreement with well-known experimental data.

ordinary–extraordinary transition | slow mode | fast mode | polyelectrolyte dynamics | polyelectrolyte aggregation

The "ordinary–extraordinary" transition has been known over the past four decades from dynamic light-scattering (DLS) experiments on aqueous solutions of charged macromolecules such as DNA, polylysine, polystyrene sulfonate, polyvinyl pyridine, etc. (1–22). In the so-called "ordinary" behavior, the diffusion coefficient D determined from DLS increases, from the value D_{SE} expected from the Stokes–Einstein law for dilute polyelectrolyte solutions at high enough monovalent salt concentrations c_s sufficient to screen electrostatic interactions, to even higher values upon a decrease in c_s. This observation is already intriguing, because the chain swells due to stronger intrachain electrostatic repulsion at lower values of c_s and hence D is expected to decrease according to the Stoke–Einstein law. However, D actually increases! Even more strangely, upon further decrease in c_s, an additional diffusion coefficient with very small values emerges, suggesting the presence of large aggregates. It is surprising that similarly charged, and hence electrostatically repulsive, polymers would aggregate at all and that they would break apart when electrostatic repulsion is screened by added electrolyte. In view of this mysterious nature, this behavior is called "extraordinary." In addition to these tantalizing facts, the occurrence of the ordinary–extraordinary behavior for solutions of charged macromolecules completely undermines the utility of the Stokes–Einstein law, which is the routine methodology for characterizing uncharged macromolecules in solutions.

The diffusional modes corresponding to the ordinary and extraordinary behaviors are also called "fast" and "slow" modes, with their respective diffusion coefficients D_f and D_s. The diffusion coefficients D_f and D_s, collected from literature originating from many laboratories worldwide (1, 11, 15, 16), are given in Fig. 1 as functions of polymer concentration c and degree of polymerization N. In addition to the abovementioned puzzles, several features characterize the ubiquitous and intriguing simultaneous occurrence of the fast and slow modes.

The fast diffusion coefficient D_f is several orders of magnitude higher than the expected value D_{SE} from its size based on the Stokes–Einstein law. Remarkably, D_f for c above a threshold value is independent of c and N over several orders of magnitude. Even more remarkably, D_f of say 10^6 Da sodium polystyrene(sulfonate) is only a factor of 4 smaller than the diffusion coefficient of a metallic ion such as K^+, Na^+, etc. As mentioned above, the fast mode behavior is called ordinary because, upon addition of small molecular salt such as NaCl, D_f decreases continuously with salt concentration c_s, eventually reaching D_{SE}.

The slow diffusion coefficient D_s is several orders of magnitude smaller than D_f and D_{SE} and it decreases strongly with an increase in either c or N. Using the Stokes–Einstein law, D_s has been interpreted in the literature with the conjecture of formation of large aggregates made of many chains. Such clustering is also seen in suspensions of charged colloidal particles and worm-like micelles (22). Concomitant to the onset of the slow mode, the scattering intensity at very small scattering angles appears to diverge (10), consistent with the conjecture of formation of aggregates (20). Upon addition of salt ($c_s > c$), the slow mode disappears. As already mentioned, this extraordinary behavior of aggregation among self-repelling chains is enigmatic. The junction point at which one diffusive mode (fast) splits into two modes (fast and slow), either when c_s is reduced or c is increased, is identified as the ordinary–extraordinary transition point. This paper provides a theory of the ordinary–extraordinary phenomenon of charged macromolecules in solutions.

Results

The resolution of these puzzles lies in the omnipresent cloud of counterions that surrounds the polymer chains (23, 24). Due to an optimization between translational entropy of counterions and attraction between the polymer and counterions, there is a net amount of counterions adsorbed around each chain, making a counterion worm (Fig. 2*A*), and indeed the effective charge of

Significance

The experimentally observed phenomenon of the "ordinary–extraordinary" transition from dynamic light-scattering measurements of solutions of charged macromolecules has remained mysterious for the past four decades and has prohibited the use of the Stokes–Einstein law in characterizing the sizes of charged polymers, using light-scattering techniques. The diffusion coefficients of polymers with molecular weight of about 1 million can be merely one-fourth of those of metallic ions such as K^+, independent of polymer molecular weight and concentration. Similarly charged macromolecules can clump together to make aggregates when electrostatic repulsion between them is dominant and they break apart when the electrostatics are screened. A theory based on counterion dynamics and dipolar interactions is presented in resolving these mysteries.

Author contributions: M.M. designed research, performed research, analyzed data, and wrote the paper.

The author declares no conflict of interest.

This article is a PNAS Direct Submission.

[1]Email: muthu@polysci.umass.edu.

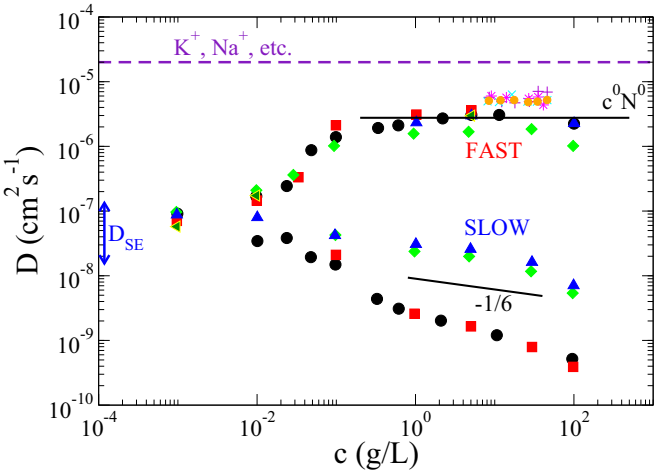

Fig. 1. Collected data on diffusion coefficient for the fast (ordinary) mode, D_f, and the slow (extraordinary) mode, D_s. The fast and slow modes emerge for polymer concentrations above a threshold value. For the fully developed two-mode regime, D_f is independent of polymer concentration c and degree of polymerization N over several orders of magnitude and is only about a factor of 4 smaller than the diffusion coefficient of a metallic ion such as Na^+ in water. D_s is smaller than D_f by three orders of magnitude and it depends on c and N, suggesting formation of aggregates by similarly charged polymers. Upon addition of electrolytes, the slow mode disappears and D_f progressively becomes smaller, approaching eventually the diffusion coefficient D_{SE} expected from the Stokes–Einstein law. Blue triangle, green diamond, red square, black circle, and green triangle data are from Förster et al. (11) for quarternized poly(2-vinylpyridine) with molecular weight $M = 1.09\times10^5$ g/mol, 2×10^5 g/mol, 7.8×10^5 g/mol, 5.8×10^5 g/mol, and 2.26×10^6 g/mol and degree of quarternization $q = 0.65$, 0.98, 0.75, 0.4, and 1.0, respectively. Purple plus, aqua cross, purple star, and gold circle data are from Sedlak and Amis (15) for sodium poly(styrene sulfonate) with $M = 5\times10^3$ g/mol, 3.82×10^4 g/mol, 1.0×10^5 g/mol, and 1.2×10^6 g/mol, respectively. The solid lines represent predictions from the present theory.

the chain is reduced from its chemical charge (23, 24). As a result, the chains do not move independently. Their dynamics are coupled to those of the counterion cloud. Therefore, direct implementation of the Stokes–Einstein law enunciated for isolated ions is not allowed in describing the dynamics of charged macromolecules. The coupled dynamics of the chains and their counterion clouds must be treated self-consistently, and proper description of the independence of electrophoretic mobility on molar mass of charged macromolecules must be taken into account (25–27). As shown below, these considerations lead to the observed fast diffusion behavior. Furthermore, when a counterion adsorbs on the polymer chain, it makes a strong dipole (23, 24). Although these dipoles are individually transients, simultaneous occurrence of several dipole–dipole pairings can result in microgel-like aggregates (Fig. 2*B*). As shown below, such dipole-mediated aggregates, originating from adsorbed counterions, are responsible for the extraordinary behavior associated with the slow mode.

Fast Mode. The diffusion coefficients given in Fig. 1 are obtained from DLS by analyzing the time dependence of the monomer density correlation function $\langle\rho_{\mathbf{k}}(t)\rho_{-\mathbf{k}}(0)\rangle$, where the Fourier transform of the local monomer density is defined as (28, 29)

$$\rho_{\mathbf{k}}(t) = \frac{1}{V}\sum_{\beta j} e^{i\mathbf{k}\cdot\mathbf{R}_{\beta j}(t)}. \qquad [1]$$

The whole system consists of n polyelectrolyte chains of uniform length $N\ell$, with N Kuhn segments of length ℓ, dispersed in a polar solvent of volume V containing fully dissociated salt at concentration c_s. The average polymer concentration is $c = nN/V$. Each monomer of the chains is ionizable and the ionized groups are assumed to be uniformly distributed along the chain with α as the average degree of ionization. The concentration of the monovalent counterions arising from the dissociated monomers is $\alpha z_p c$, where z_p is the number of ionizable groups per Kuhn segment. $\mathbf{R}_{\beta j}(t)$ is the position vector at time t of the jth monomer of the βth chain ($1\le j\le N, 1\le\beta\le n$). $\mathbf{k}$ is the scattering wave vector. Using the standard theory of polymer dynamics (25–31), the time evolution of $\rho_{\mathbf{k}}(t)$ is given by

$$\frac{\partial\rho_{\mathbf{k}}(t)}{\partial t} = -\Gamma_k\rho_{\mathbf{k}} + f_{\mathbf{k}}, \qquad [2]$$

where $f_{\mathbf{k}}$ is the white noise satisfying the fluctuation–dissipation theorem and

$$\Gamma_k = k_BT\int\frac{d^3q}{(2\pi)^3}\,\frac{\mathbf{k}\cdot(1-\hat{\mathbf{q}}\hat{\mathbf{q}})\cdot\mathbf{k}}{\eta_0\left(q^2+\xi_h^{-2}\right)}\,\frac{g(\mathbf{k}+\mathbf{q})}{g(\mathbf{k})}. \qquad [3]$$

Here, k_BT is the Boltzmann constant times the absolute temperature, ξ_h is the hydrodynamic screening length (27), and the scattering function per segment is (32)

$$g(\mathbf{k}) = \frac{V}{c}\langle\rho_{\mathbf{k}}(t)\rho_{-\mathbf{k}}(t)\rangle. \qquad [4]$$

For polyelectrolyte solutions, where monomer density fluctuations are strongly correlated by long-ranged electrostatic interactions, $g(\mathbf{k})$ is a complicated function of c and c_s, depending on three quantities, v, w_c, and κ: excluded volume parameter $v = (1/2-\chi)\ell^3$, where χ is the Flory–Huggins parameter for solvent–polymer backbone interaction (33); strength of the segment–segment electrostatic interaction (34) $w_c = 4\pi\alpha^2 z_p^2\ell_B$, where ℓ_B is the Bjerrum length $e^2/(4\pi\epsilon_0\epsilon k_BT)$ ($e =$ the electronic charge, $\epsilon_0 =$ permittivity of vacuum, and $\epsilon =$ dielectric constant of the solution); and range of electrostatic interaction given by the Debye length $\kappa^{-1} = [4\pi\ell_B(\alpha z_p c + 2c_s)]^{-1/2}$, where the counterions and dissociated salt ions are taken as monovalent. Analytical results emerge in the asymptotic limits of low salt ($\kappa\to0$) and high salt ($\kappa^2\ell^2 \gg 1$). In the high-salt limit, $g(\mathbf{k})$ is the same as for solutions of uncharged polymers (with v replaced by $v + w_c/\kappa^2$), decreasing monotonically with k.

In the low-salt limit, $g(\mathbf{k})$ is nonmonotonic in k and exhibits the "polyelectrolyte peak" at k_m for all polyelectrolyte concentrations

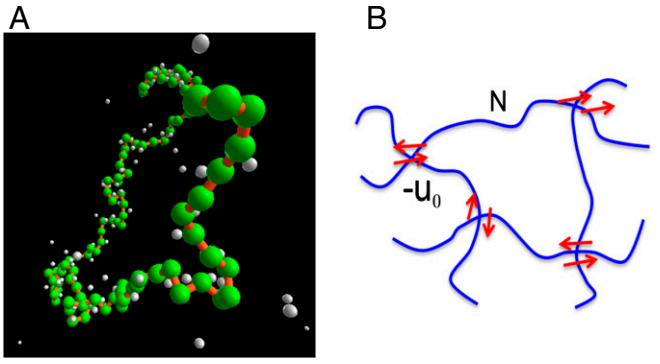

Fig. 2. (*A*) Counterion cloud (white) surrounding a polyelectrolyte chain (green). The coupled dynamics of the chains and their counterion clouds are measured in the fast mode. (*B*) Cartoon of several dipole–dipole pairings responsible for microgel-like aggregate formation attributed to the slow mode. Each red arrow denotes a dipole formed by an adsorbed counterion on the polymer backbone. u_0 is the magnitude of the average attractive energy between two adjacent dipoles in contact, averaged over different favorable orientations. N is the number of segments between two such physical cross-links.

(1, 5, 10, 35–48). For c less than the overlap concentration c^*, $g(\mathbf{k})$ is the product of the form factor $P(k)$ and intermolecular structure factor $S_{int}(\mathbf{k})$,

$$g(\mathbf{k}) = P(k)S_{int}(\mathbf{k}), \quad [5]$$

where $P(k) = (1 - k^2R_g^2/3 + \cdots)$ for $kR_g \ll 1$ and $P(k) \sim k^{-\nu}$ for $kR_g \gg 1$, with R_g being the radius of gyration of a chain, and ν is the size exponent given by $R_g \sim N^{\nu}$. For infinitely dilute solutions, so dilute that the chains are not electrostatically correlated, the intermolecular structure factor exhibits a scattering peak at $k_m \sim c^{1/3}$ as a manifestation of average interchain distance given geometrically by $c^{-1/3}$. When c is increased, but still in dilute regime, the chains are electrostatically correlated with their average separation distance given by the Debye length κ^{-1} ($\sim c^{-1/2}$ for $c_s = 0$). Therefore, $k_m \sim c^{1/2}$. For $c \geq c^*$, the chains interpenetrate and are correlated both electrostatically and topologically, resulting in a coupled double screening (Edwards screening and Debye–Hückel screening) (25). Now, $g(\mathbf{k})$ is of the form

$$g(\mathbf{k}) = \frac{1}{cw_c}\,\frac{k^2}{\left(1 + k^4\xi^4\right)}, \quad [6]$$

where $\xi \sim c^{-1/2}$ for semidilute solutions (where concentration fluctuations are strong) and $\xi \sim c^{-1/4}$ for concentrated solutions (where concentration fluctuations are weak). Therefore, $g(\mathbf{k})$ exhibits a peak at $k_m \sim c^{1/2}$ for semidilute solutions and at $k_m \sim c^{1/4}$ for concentrated solutions. Thus, in the low-salt limit, four regimes of polyelectrolyte concentration may be identified and in each regime, $g(\mathbf{k})$ exhibits a peak at k_m: (*i*) infinitely dilute and electrostatically uncorrelated, $k_m \sim c^{1/3}$; (*ii*) dilute and electrostatically correlated, $k_m \sim c^{1/2}$; (*iii*) semidilute with strong concentration fluctuations, $k_m \sim c^{1/2}$; and (*iv*) concentrated with weak concentration fluctuations, $k_m \sim c^{1/4}$. Substitution of these results in Eqs. **2** and **3** yields expressions for the diffusion coefficient.

For the high-salt limit, as $g(\mathbf{k})$ is a monotonically decaying function of k, Γ_k is diffusive for small k,

$$\Gamma_k = D_c k^2 + 0\left(k^4\right), \quad [7]$$

where D_c is the cooperative diffusion coefficient. Now D_c is proportional to R_g^{-1} for dilute solutions ($c < c^*$) and to ξ^{-1} for $c > c^*$. For salt-free conditions, in view of $g(\mathbf{k})$ of Eq. **6** being $\sim k^2$ for small k, Γ_k is not purely diffusive,

$$\Gamma_k = \Gamma_0 + D_c k^2 + 0\left(k^4\right), \quad [8]$$

where $\Gamma_0 \sim \xi^{-3}$ and $D_c \sim \xi^{-1}$.

In addition to the cooperative diffusion addressed in the above equations, the local motion of monomers is coupled to the dynamics of the counterions in the neighborhood of the monomers (29). The counterion cloud generates an electric field $\mathbf{E}$ on the monomer, and as a result there is an additional convective contribution to the flux, $\rho\mu_0\mathbf{E}$, where μ_0 is the monomer electrophoretic mobility α/ζ_0 (ζ_0 is the monomer friction coefficient). Inclusion of this coupling, to leading order in monomer density, into the continuity equation of Eq. **2** gives

$$\frac{\partial \rho_{\mathbf{k}}(t)}{\partial t} = -\Gamma_k \rho_{\mathbf{k}} - \mu_0 z_p c(i\mathbf{k}\cdot\mathbf{E}). \quad [9]$$

Now, according to Poisson's equation

$$i\mathbf{k}\cdot\mathbf{E} = \frac{1}{\epsilon_0\epsilon}\left(\alpha\rho_{\mathbf{k}} + z_c\rho_{c,\mathbf{k}}\right) \quad [10]$$

for salt-free solutions, where ρ_c is the local concentration of counterions (of valency z_c). Therefore, the time evolution of $\rho_{\mathbf{k}}$ is coupled to ρ_c. Analogous to Eq. **9**, the time evolution of $\rho_{c,\mathbf{k}}$ can be written as

$$\frac{\partial \rho_{c,\mathbf{k}}}{\partial t} = -D'k^2\rho_{c,\mathbf{k}} - \frac{\mu' c_c}{\epsilon_0\epsilon}\left(\alpha\rho_{\mathbf{k}} + z_c\rho_{c,\mathbf{k}}\right), \quad [11]$$

where $c_c = \alpha c/z_c$, and D' and $\mu' = z_c D'/(k_B T)$ are the diffusion coefficient and electrophoretic mobility of the counterion, respectively. Due to the coupling of $\rho_{\mathbf{k}}$ and $\rho_{c,\mathbf{k}}$, there are two decay rates, which we label as superfast and fast modes. If there are additional charged species, there will be additional modes.

As we anticipate that the fluctuation in the counterion distribution would come to equilibrium more rapidly than the macromolecule (29), we can approximate $\partial\rho_{c,\mathbf{k}}/\partial t \sim 0$. This enables an analytical expression for $\partial\rho_{\mathbf{k}}/\partial t$ as

$$\frac{\partial \rho_{\mathbf{k}}}{\partial t} = -\Gamma_0\rho_{\mathbf{k}} - D_c k^2\rho_{\mathbf{k}} - \frac{c\mu_0\alpha z_p e}{\epsilon_0\epsilon\left(k^2 + \kappa^2\right)}k^2\rho_{\mathbf{k}}. \quad [12]$$

For small $k < \kappa$, this becomes

$$\frac{\partial \rho_{\mathbf{k}}}{\partial t} = -\Gamma_0\rho_{\mathbf{k}} - D_f k^2\rho_{\mathbf{k}}, \quad [13]$$

where the fast diffusion coefficient is given as

$$D_f = D_c + \frac{c\mu_0\alpha z_p e}{\epsilon_0\epsilon\kappa^2}. \quad [14]$$

Noting that $\mu_0 = e\alpha/\zeta_0$, $\kappa^2 = e^2\alpha z_p c z_c^2/(\epsilon_0\epsilon k_B T)$, and $z_c = 1$ for monovalent counterions,

$$D_f = D_c + \alpha D_0, \quad [15]$$

where $D_0 = k_B T/\zeta_0$ is the monomer diffusion coefficient. Because D_c of a macromolecule is orders of magnitude smaller than the monomer diffusion coefficient (if the monomer were to be alone and not a part of the chain), the fast diffusion coefficient is predicted as

$$D_f \simeq \alpha D_0, \quad \text{independent of } N \text{ and } c. \quad [16]$$

As the effective degree of ionization is about 0.25–0.3 due to counterion adsorption, and taking D_0 as that of a metallic ion, the fast diffusion coefficient is about 5×10^{-6} cm^2/s as seen in Fig. 1. The derived theory of D_f as the renormalized D_c is also of relevance to other systems such as critical fluids, colloidal suspensions, gels, etc.

Slow Mode. When two dipoles $\mathbf{p}_1$ and $\mathbf{p}_2$, each constituted by a monomer charge and its adsorbed counterion, are oriented either parallel or antiparallel, their interaction energy $U(r)$ is attractive given by $-p_1p_2\ell_B k_B T f(\kappa r)/r^4$, where $f(\kappa r)$ is a known function. If these dipoles are randomly oriented, the interaction energy is

$$\frac{U(r)}{k_B T} = -\frac{p_1^2 p_2^2 \ell_B^2}{r^6}e^{-2\kappa r}\left[1 + 2\kappa r + \frac{5}{3}(\kappa r)^2 + \frac{2}{3}(\kappa r)^3 + \frac{1}{6}(\kappa r)^4\right]. \quad [17]$$

As a typical example, $U(r) \sim -10k_B T$ if the separation distance between the dipoles and the dipole length are 0.25 nm, comparable to the monomer separation distance along the chain for salt-free water at room temperature. If we define the Flory–Huggins parameter χ_{dipole} as a contact potential arising from pairwise dipolar interaction according to

$$\left(\frac{1}{2} - \chi_{\text{dipole}}\right) \equiv -u_0 = \frac{1}{\ell^3}\int d\mathbf{r}\left[1 - e^{-U(r)/k_B T}\right], \quad [18]$$

then $(1/2 - \chi_{\text{dipole}})$ is -12.6 at $c_s = 10^{-4}$ M, showing that χ_{dipole} is enormously positive due to such dipolar attractions.

Due to such strong attractive contact energy between two dipoles (constituted by adsorbed counterions on charged monomers), we allow aggregation of m uniformly charged chains (Fig. 2*B*). The standard theory (49) of micellization gives the mole fraction of m-mers as

$$X_m = m\left[X_1 e^{(1/k_BT)(F_1 - F_m/m)}\right]^m, \quad [19]$$

for a fixed mole fraction of the polymer, $X = \sum_{m=1}^{\infty} X_m$. Here, X_1 and F_1 are the mole fraction and free energy of unaggregated unimer, and F_m is the free energy of the m-mer.

Consider a microgel with m chains, each of N segments, with polymer volume fraction ϕ inside the microgel. The free energy of this system is given by the classical theory of Flory (33) as

$$\frac{F_m}{k_BT} = mN\left[\left(\frac{1}{2}-\chi\right)\phi + \frac{1}{6}\phi^2 + \cdots\right] + \frac{3m}{2}\left[N^{-1/3}\phi^{-2/3} + \frac{1}{3}\ln\phi\right] + \left[\sqrt{\alpha^2 m^2 N^2 + 4n_s^2} - 2n_s\right]\ln\phi - \frac{m}{2}u_0, \quad [20]$$

where the first three terms on the right-hand side arise from the thermodynamic theory of free energy of mixing, rubber elasticity theory, and excess osmotic pressure inside the microgel (Donnan equilibrium of dissociated ions), respectively. The last term denotes the attractive energy arising from the dipolar junctions (u_0 is the strength of the contact energy, $m/2$ is the number of junctions in accordance with Flory's mean-field theory, χ is the Flory–Huggins parameter for the solvent quality, and $2n_s$ is the number of dissociated salt ions inside the microgel. In general, N can depend on polymer concentration for physical microgels. Eq. **20** is minimized with respect to ϕ and F_m is calculated for the equilibrated microgel.

For salt-free conditions, the equilibrium polyelectrolyte concentration of the microgel is

$$\phi^{-2/3} = N^{4/3}\left(\alpha + \frac{1}{2N}\right), \quad [21]$$

and F_m becomes

$$\frac{F_m}{mk_BT} = -\frac{u_0}{2} + \frac{3N}{2}\left(\alpha + \frac{1}{2N}\right)\left\{1 - \ln\left[N^{4/3}\left(\alpha + \frac{1}{2N}\right)\right]\right\}, \quad [22]$$

apart from a constant term. The free energy of the unimer is given for salt-free conditions as (34)

$$\frac{F_1}{k_BT} = 1.11\left(\frac{\alpha^2\ell_B}{\ell}\right)^{2/3} N. \quad [23]$$

Combining the above two equations gives

$$\frac{F_1}{k_BT} - \frac{F_m}{mk_BT} = \left(1 - \frac{1}{m}\right)\theta, \quad [24]$$

where θ is given by

$$\theta = 1.11\left(\frac{\alpha^2\ell_B}{\ell}\right)^{2/3} + \frac{u_0}{2} - \frac{3N\alpha}{2}\left[1 - \ln\left(N^{4/3}\alpha\right)\right], \quad [25]$$

where $1/2N$ is neglected in comparison with the degree of ionization α. The mole fraction of m-mers follows from Eqs. **19** and **24** as

$$X_m = m\left(X_1 e^{\theta}\right)^m e^{-\theta}, \quad [26]$$

with the constraint $X = \sum_{m=1}^{\infty} X_m$. As well known (49), the above equation shows that there exists a critical aggregation concentration (CAC), $X_{\mathrm{CAC}} = e^{-\theta}$, above which m-mers will form spontaneously. As a typical example, the dependence of X_1 on X is given in Fig. 3*A* for $\alpha = 0.3$, $\ell_B/\ell = 3$, $u_0 = 10$, and $N = 16$. For this set of values, $X_{\mathrm{CAC}} = 8.68 \times 10^{-11}$. If the molecular weight of the polyelectrolyte is 350,000 g/mol, then $X = 5.148 \times 10^{-8}$ is equivalent to the polymer concentration of 1 g/L. Therefore, CAC is 1.686×10^{-3} g/L. The distribution of X_m is given in Fig. 3*B* for polymer concentrations of 1 g/L. It can be readily shown that the average size of the aggregate increases with polymer concentration. The functional form of Eq. **26**, where θ is independent of m, enables several general conclusions on the size distribution (49). For $c >$ CAC and for large m,

$$X_m \sim m e^{-\left(m/\sqrt{Xe^{\theta}}\right)} \quad [27]$$

$$m_{\max} = \sqrt{X} e^{\theta/2} \quad [28]$$

$$\langle m \rangle = 2\sqrt{X} e^{\theta/2} \quad [29]$$

$$\langle m^2 \rangle - \langle m^2 \rangle = 2Xe^{\theta/2}, \quad [30]$$

where $m_{\max}$ is the number of chains in the microgel at which X_m is maximum, $\langle m \rangle$ is the average number of chains in the aggregate, and $\langle m^2 \rangle - \langle m \rangle^2$ is the SD. By writing the volume fraction of the equilibrated microgel as $\langle m \rangle N\ell^3/((4/3)\pi R_{\mathrm{agg}}^3)$, it follows from Eqs. **21** and **29** that

$$R_{\mathrm{agg}} = \left(\frac{3}{2\pi}\right)^{1/3} N\sqrt{\alpha} e^{\theta/6} X^{1/6} \sim c^{1/6}. \quad [31]$$

Substituting this into the Stokes–Einstein expression for the self-diffusion coefficient of the aggregate gives

$$D_{\mathrm{agg}} \sim \frac{T}{\eta_0 c^{1/6}}. \quad [32]$$

This mean-field result is included in Fig. 1 as a theoretical expectation. Because the slow mode is here associated with diffusion of aggregates, the onset of the slow mode is correlated with the CAC. In other words, to observe the slow mode in DLS, it is necessary for the polymer concentration to be higher than the CAC.

Discussion

The fast (ordinary) mode is shown to arise from the coupling between dynamics of polymer segments and their counterion

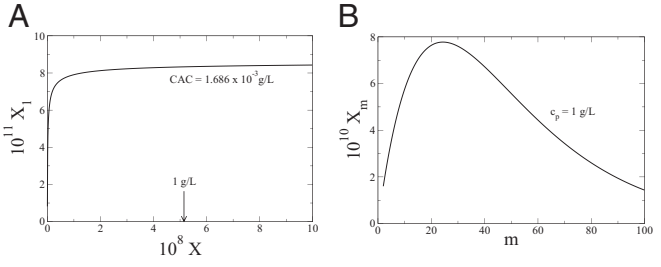

Fig. 3. (*A*) Dependence of mole fraction of unaggregated chains on the total mole fraction of the polymer in the salt-free solution for $\alpha = 0$, $\ell_B/\ell = 3$, $u_0 = 10$, and $N = 16$. For $M = 350{,}000$ g/mol, $X = 5.148 \times 10^{-8}$ is equivalent to the total polymer concentration of 1 g/L, which is orders of magnitude higher than the CAC of 1.686×10^{-3} g/L. (*B*) Distribution function of the mole fraction of m-mers for polymer concentration of 1 g/L.

cloud. Here, the diffusion coefficient D_f is the sum of the cooperative diffusion coefficient D_c (if there were no coupling as in uncharged polymers) and the contribution from coupling, which is simply the monomer diffusion coefficient D_0 with a prefactor of the effective degree of ionization α (Eq. **16**). Because $D_c < \alpha D_0$, D_f is about one-fourth of the diffusion coefficient of an electrolyte ion. In the presence of added salt, the expression for D_f is the same as Eq. **14** with $\kappa^2 = 4\pi\ell_B(\alpha c + 2c_s)$ for monovalent counterions and salt ions. As c_s increases the second term of Eq. **14** becomes weaker and D_f approaches D_c as seen in experiments. Even in the absence of deliberately added salt, a crossover from the asymptotic regime of $D_f \sim c^0 N^0$ to $D_f \sim D_{SE}$ is seen as the polymer concentration is reduced to very low values. At such low polymer concentrations in aqueous media, there are always impurities and dissociated ions from water, etc., acting like salt. In addition, D_c itself picks up $\sqrt{c}$ dependence because the static correlation length (exhibited by the polyelectrolyte peak) varies as $c^{-1/2}$ in dilute solutions. Our derived result is different from the classical Nernst–Hartley result (29) for coupled diffusion of electrolyte ions, with the difference arising from the fact that the electrophoretic mobility of a polyelectrolyte is independent of its molecular weight. The present theory is an extension of mode coupling (22) of mass and momentum fluctuations to include charge fluctuations.

The slow (extraordinary) mode is attributed to the formation of microgel-like aggregates where the physical cross-links arise from dipole–dipole pairings with each dipole originating from an adsorbed counterion to a charged monomer belonging to the polymer. By equilibrating such aggregates with Flory's theory of ionic gels and implementing the theory of micellization, we have established the criterion for the onset of the slow mode as the CAC. The ordinary–extraordinary transition (splitting) point is identified with CAC. For $c >$ CAC, microgel-like aggregates form and the average number of chains in the aggregates increases with polymer concentration as $\sqrt{c}$ (Eq. **29**). This in turn results in $D_{\text{app}} \sim c^{-1/6}$ as shown in Fig. 1. These results based on dipole–dipole-mediated microgel formation, originating from counterion adsorption, appear to be qualitatively consistent with the slow mode behavior. The discrepancy in quantitative details between the above law and experimental data can readily arise from polydispersity in the aggregate size, concentration dependence of cross-link density, and entanglement effects at higher polymer concentrations.

The above calculation can be repeated at high-salt concentrations. Now the equilibrium volume fraction inside the microgel is given by

$$\phi^{-1} = N^{4/5}\left(\frac{1}{2} - \chi + \frac{\alpha^2}{4v_1 c_s}\right)^{3/5}, \qquad [33]$$

where v_1 is the volume of a solvent molecule. For the high-salt limit, F_1 is given by

$$\frac{F_1}{k_B T} = 1.8\left(\frac{1}{2} - \chi + \frac{\alpha^2}{2v_1 c_s}\right)^{2/5} N^{1/5}. \qquad [34]$$

By combining Eqs. **19**, **33**, and **34**, the expression for θ in Eq. **26** is replaced by (for $\chi = 1/2$)

$$\theta = \frac{u_0}{2} + N^{1/5}\left(\frac{\alpha^2}{4v_1 c_s}\right)^{2/5}\left[0.8752 + \frac{3}{5}\ln\left(\frac{N^{4/3}\alpha^2}{4v_1 c_s}\right)\right]. \qquad [35]$$

The general conclusions given in Eqs. **27**–**30** are still the same except that the CAC is very high. For example, for $\alpha = 0.1$, $N = 16$, $\ell_B/\ell = 3$, $u_0 = 9$, and $c_s = 0.1$ M [by taking $v_1 = (0.23\ \text{nm})^3$], CAC = 4.017 g/L. Even for the unphysically large polymer concentration of 100 g/L, $m_{\max}$ is only 4. In fact, this theory predicts that CAC(c_s)/CAC($c_s = 0$) = 15, 2,382, and 81,600 for c_s = 0.05 M, 0.1 M, and 0.2 M, respectively. Full crossover formulas need to be used in comparing with experiments at moderate c_s values, instead of the asymptotic formulas mentioned here. Nevertheless, such a strong increase in polymer concentration for the onset of slow mode as the salt concentration is increased is qualitatively consistent with experimental data.

It should be noted that the model presented here for the slow mode is analogous to the aggregation phenomenon in gelation of associating uncharged polymers (50–52). In these studies, the focus is the competition between sol-gel transition and liquid–liquid phase separation, whereas the present focus is far away from the macroscopic sol-gel transition. Also, using a combinatorics analysis of associating polymers, the authors of ref. 48 have shown that the system of reversibly associating polymers is correctly described by the Flory theory that is used here. Of particular relevance is the simulation study (49, 50) showing that micelle-like structures form if pairwise association energy is above a threshold value. However, for these structures to contribute dynamically, there is another threshold value beyond which chain dynamics are essentially frozen. Consistent with this picture, the present model assumes that the association energy is sufficiently strong such that micelle-like structures are allowed and at the same time the diffusion time of a chain in the aggregate is longer than the lifetime of the aggregate. Ermoshkin and de la Cruz (53, 54) have extended the theory of ref. 48 to treat polyelectrolyte gels created by divalent ions, with the main focus being sol-gel transition and liquid–liquid phase separation. Because the combinatorics treatment of associating bonds is equivalent to the Flory model, the new element is the concentration fluctuations, which are also treated in other works using replica formalism and charge regularization (55, 56). The relative merits of these advances are yet to be explored. In general, the slow mode treated here occurs at experimental conditions far from the sol-gel transition addressed in the abovementioned theories.

It must be mentioned that the mechanism proposed here for aggregation of similarly charged polymers, mediated by dipoles originating from adsorbed counterions, is of general applicability even beyond the presently treated charged homopolymers in polar solvents.

Materials and Methods

The derivations use well-established theoretical methods in polymer physics. The fast mode is addressed with a combination of the Onsager equation, Rouse–Zimm equations, field theory, and fluctuation–dissipation theory. The slow mode is addressed with a combination of dipole–dipole interaction energy, Flory's theory of ionic gels, and micellization theory.

ACKNOWLEDGMENTS. The author acknowledges numerous stimulating discussions with Manfred Schmidt on this difficult subject. Acknowledgment is made to the National Science Foundation (Grant DMR 1404940), the National Institutes of Health (Grant R01HG002776-11), and Air Force Office of Scientific Research (Grant FA9550-14-1-0164).

1. Förster S, Schmidt M (1995) Polyelectrolytes in solution. *Adv Polym Sci* 120: 51–133.
2. Jamieson AM, Presley CT (1973) Anisotropic translational diffusion in dilute aqueous solutions of partially hydrolyzed polyacrylamide by quasielastic light scattering. *Macromolecules* 6(3):358–360.
3. Lin S, Lee W, Schurr J (1978) Brownian motion of highly charged poly(l-lysine). Effects of salt and polyion concentration. *Biopolymers* 17:1041–1064.
4. Wilcoxon J, Schurr J (1983) Electrophoretic light scattering studies of poly(l-lysine) in the ordinary and extraordinary phase. Effects of salt, molecular weight, and polyion concentration. *J Chem Phys* 78(6):3354–3364.
5. Drifford M, Dalbiez JP (1984) Light scattering by dilute solutions of salt-free polyelectrolytes. *J Phys Chem* 88:5368–5375.
6. Drifford M, Dalbiez JP (1985) Effect of salt on sodium polystyrene sulfonate measured by light scattering. *Biopolymers* 24:1501–1514.

7. Ramsay D, Schmitz K (1985) Quasi-elastic light scattering and fluorescence photobleaching recovery studies on poly(lysine) dynamics. *Macromolecules* 18:2422–2429.
8. Schurr J, Schmitz K (1986) Dynamic light scattering studies of biopolymers: Effects of charge, shape, and flexibility. *Annu Rev Phys Chem* 37:271–305.
9. Sedlak M, Konak C, Jakes J (1987) Semidilute solutions of poly(methacrylic acid) in the absence of salt: Dynamic light scattering study. *Polymer* 28:873–880.
10. Schmidt M (1989) Static and dynamic light scattering by an aqueous polyelectrolyte solution without added salt: Quarternized poly(2-vinylpyridine). *Macromol Chem Rapid Commun* 10(2):89–96.
11. Förster S, Schmidt M, Antonietti M (1990) Static and dynamic light scattering by aqueous polyelectrolyte solutions: Effect of molecular weight, charge density and added salt. *Polymer* 31:781–792.
12. Ghosh S, Li X, Reed C, Reed W (1990) Apparent persistence lengths and diffusion behavior of high molecular weight hyaluronate. *Biopolymers* 30:1101–1112.
13. Ghosh S, Peitzsch RM, Reed WF (1992) Aggregates and other particles as the origin of the "extraordinary" diffusional phase in polyelectrolyte solutions. *Biopolymers* 32: 1105–1122.
14. Peitzsch RM, Burt MJ, Reed WF (1992) Evidence of partial draining for linear polyelectrolytes: Heparin, chondroitin 6-sulfate, and poly(styrenesulfonate). *Macromolecules* 25: 806–815.
15. Sedlak M, Amis EJ (1992) Dynamics of moderately concentrated salt-free polyelectrolyte solutions: Molecular weight dependence. *J Chem Phys* 96:817–825.
16. Sedlak M, Amis EJ (1992) Concentration and molecular weight regime diagram of salt-free polyelectrolyte solutions as studied by light scattering. *J Chem Phys* 96: 826–834.
17. Sedlak M (1993) Domain structure of polyelectrolyte solutions: Is it real? *Macromolecules* 26:1158–1162.
18. Sedlak M (1996) The ionic strength dependence of the structure and dynamics of polyelectrolyte solutions as seen by light scattering: The slow mode dilemma. *J Chem Phys* 105:10123–10133.
19. Smits RG, Kuil ME, Mandel M (1993) Molar mass and ionic strength dependence of the apparent diffusion coefficient of a flexible polyelectrolyte at dilute and semidilute concentrations: Linear poly(ethylenimine). *Macromolecules* 28:2315–2328.
20. Zhang Y, Douglas JF, Ermis BD, Amis EJ (2001) Influence of counterion valency on the scattering properties of highly charged polyelectrolyte solutions. *J Chem Phys* 114: 3299.
21. Zhou K, et al. (2009) Re-examination of dynamics of polyelectrolytes in salt-free dilute solutions by designing and using a novel neutral-charged-neutral reversible polymer. *Macromolecules* 42(18):7146–7154.
22. Schmitz KS (1993) *Macroions in Solution and Colloidal Suspension* (VCH Publishers, New York).
23. Liu S, Muthukumar M (2002) Langevin dynamics simulation of counterion distribution around isolated flexible polyelectrolyte chains. *J Chem Phys* 116:9975–9982.
24. Muthukumar M (2004) Theory of counter-ion condensation on flexible polyelectrolytes: Adsorption mechanism. *J Chem Phys* 120(19):9343–9350.
25. Muthukumar M (1996) Double screening in polyelectrolyte solutions: Limiting laws and crossover formulas. *J Chem Phys* 105:5183–5199.
26. Muthukumar M (1996) Theory of electrophoretic mobility of a polyelectrolyte in semidilute solutions of neutral polymers. *Electrophoresis* 17(6):1167–1172.
27. Muthukumar M (1997) Dynamics of polyelectrolyte solutions. *J Chem Phys* 107: 2619–2635.
28. Doi M, Edwards SF (1986) *The Theory of Polymer Dynamics* (Clarendon, Oxford).
29. Berne BJ, Pecora R (1976) *Dynamic Light Scattering* (Dover, New York).
30. Vilgis TA, Borsali R (1991) Mean-field theory of concentrated polyelectrolyte solutions: Statics and dynamics. *Phys Rev A* 43(12):6857–6874.
31. Ajdari A, Leibler L, Joanny JF (1991) Cooperative diffusion in weakly charged polyelectrolyte solutions. *J Chem Phys* 95:4580–4583.
32. Higgins JS, Benoit HC (1994) *Polymers and Neutron Scattering* (Clarendon, Oxford).
33. Flory PJ (1953) *Principles of Polymer Chemistry* (Cornell Univ Press, Ithaca, NY).
34. Muthukumar M (2011) *Polymer Translocation* (CRC, Boca Raton, FL).
35. de Gennes PG, Pincus P, Velasco RM, Brocahrd F (1976) Remarks on polyelectrolyte conformation. *J Phys* 37(12):1461–1473.
36. Nierlich M, et al. (1979) Small angle neutron scattering by semi-dilute solutions of polyelectrolyte. *J Phys* 40:701–704.
37. Nallet F, Jannink G, Hayter JB, Oberthür R, Picot C (1983) Observation of the dynamics of polyelectrolyte strong solutions by quasi-elastic neutron scattering. *J Phys* 44(1): 87–99.
38. Jannink G (1986) Structure factors of polyelectrolyte solutions revealed by neutron scattering. *Macromol Symp* 1(1):67–90.
39. Kaji K, Urakawa H, Kanaya T, Kitamaru R (1988) Phase diagram of polyelectrolyte solutions. *J Phys* 49(6):993–1000.
40. Borue VY, Erukhimovich IY (1988) A statistical theory of weakly charged polyelectrolytes: Fluctuations, equation of state, and microphase separation. *Macromolecules* 21:3240–3249.
41. Krause R, et al. (1989) Static light scattering by solutions of salt-free polyelectrolytes. *Physica A* 160(2):135–147.
42. Johner C, et al. (1994) Static light scattering and electric birefringence experiments on saltfree solutions of poly(styrenesulfonate). *J Phys II* 4(9):1571–1584.
43. Nishida K, Kaji K, Kanaya T (1995) Charge density dependence of correlation length due to electrostatic repulsion in polyelectrolyte solutions. *Macromolecules* 28: 2472–2475.
44. Ermi BD, Amis EJ (1997) Influence of backbone solvation on small angle neutron scattering from polyelectrolyte solution. *Macromolecules* 30:6937–6942.
45. Nishida K, Kaji K, Kanaya T (2001) High concentration crossovers of polyelectrolyte solutions. *J Chem Phys* 114:8671–8677.
46. Prabhu VM, Muthukumar M, Wignall GD, Melnichenko YB (2001) Dimensions of polyelectrolyte chains and concentration fluctuations in semidilute solutions of sodium-poly(styrne sulfoante) as measured by small-angle neutron scattering. *Polymer* 42:8935–8946.
47. Nishida K, Kaji K, Shibano T (2002) Added salt effect on the intermolecular correlation in flexible polyelectrolyte solutions: Small-angle scattering study. *Macromolecules* 35: 4084–4089.
48. Prabhu VM, Muthukumar M, Wignall GD, Melnichenko YB (2003) Polyelectrolyte chain dimensions and concentration fluctuations near phase boundaries. *J Chem Phys* 119:4085–4098.
49. Israelachvili JN (2011) *Intermolecular and Surface Forces* (Elsevier, Amsterdam).
50. Semenov AN, Rubinstein M (1998) Thermoreversible gelation in solutions of associative polymers. 1. Statics. *Macromolecules* 31:1373–1385.
51. Kumar SK, Panagiotopoulos AZ (1999) Thermodynamics of reversibly associating polymer solutions. *Phys Rev Lett* 82:5060–5063.
52. Kumar SK, Douglas JF (2001) Gelation in physically associating polymer solutions. *Phys Rev Lett* 87:188301.
53. Ermoshkin AV, Olvera de la Cruz M (2003) Polyelectrolytes in the presence of multivalent ions: Gelation versus segregation. *Phys Rev Lett* 90(12):125504.
54. Ermoshkin AV, Olvera de la Cruz M (2004) Gelation in strongly charged polyelectrolytes. *J Polym Sci B Polym Phys* 42:766–776.
55. Muthukumar M (1989) Polyelectrolyte gels: Replica theory. *Springer Proc Phys* 42: 28–34.
56. Hua J, Mitra MK, Muthukumar M (2012) Theory of volume transition in polyelectrolyte gels with charge regularization. *J Chem Phys* 136(13):134901.